

# Benzene Alkylation with Propane over Pt-Modified MFI Zeolites

Andrei V. Smirnov,\* Evgenii V. Mazin,\* Valentina V. Yuschenko,\* Elena E. Knyazeva,\* Sergei N. Nesterenko,\* Irina I. Ivanova,\*<sup>1</sup> Leonid Galperin,† Robert Jensen,† and Steven Bradley†

\*Laboratory of Kinetics and Catalysis, Department of Chemistry, Moscow State University, Vorob'evy Gory, 117234 Moscow, Russia; and †UOP LLC, 25 East Algonquin Road, P.O. Box 5017, Des Plaines, Illinois 60017-5017

Received January 14, 2000; revised April 17, 2000; accepted April 17, 2000

Benzene alkylation with propane has been studied on acidic H-MFI zeolites with SiO<sub>2</sub>/Al<sub>2</sub>O<sub>3</sub> ratios of 51, 104, and 325, mixed (H-MFI + Pt/CeO<sub>2</sub>) catalytic systems, and Pt/H-MFI bifunctional catalysts with Pt content of 0.02 and 0.3%. In some of the experiments, Zr<sub>2</sub>Fe intermetallic compound was added to the catalytic system to ensure H<sub>2</sub> removal from the reaction zone. The reaction was carried out at atmospheric pressure, in the temperature range of 573–773 K, C<sub>3</sub>H<sub>8</sub>/C<sub>6</sub>H<sub>6</sub> = 1, and WHSV = 0.2–7 h<sup>-1</sup>. The conversion of propane and selectivity to propylbenzenes was found to increase in the following order of catalytic systems: H-MFI < (H-MFI + Pt/CeO<sub>2</sub>) < Pt/H-MFI < (Pt/H-MFI + Zr<sub>2</sub>Fe). The increase of the number of strong Brønsted sites in zeolite led, on one hand, to the increase of propane conversion, but on the other hand, to the decrease of the selectivity to target products, which was due to the cracking of propane and propylbenzenes dealkylation and dismutation. Incorporation of Pt into the catalytic system enhanced propane dehydrogenation at the expense of its cracking and resulted in significant improvement of propane conversion and selectivity to propylbenzenes. Addition of an H<sub>2</sub> scavenger allowed a shift of the thermodynamic equilibria and an increase in propane and benzene conversion. The best result was obtained on the (Pt/H-MFI + Zr<sub>2</sub>Fe) catalytic system with an SiO<sub>2</sub>/Al<sub>2</sub>O<sub>3</sub> ratio of 325 and a Pt content of 0.22%, on which the yield of propylbenzenes reached 96% with respect to equilibrium and selectivity to propylbenzenes was about 60%. The mechanisms of benzene alkylation with propane operating on various catalysts are discussed. © 2000 Academic Press

**Key Words:** alkylation with alkanes; propylbenzenes; propane activation; MFI zeolites; Pt-supported catalysts; H<sub>2</sub> scavengers.

## INTRODUCTION

Light alkanes such as methane, ethane, propane, and butanes are among the most abundant and inexpensive hydrocarbons available today. Until now there has been no efficient commercial process for light alkanes functionalization, and therefore such a route would represent superior useful technology for the utilization of natural gas and similar refinery-derived light hydrocarbon streams (1). One possible way to upgrade light alkanes is to involve them in

reactions with other organic molecules, for example, in the alkylation of aromatic hydrocarbons.

The use of both light alkanes and aromatics as raw materials in a common process can lead to valuable products and intermediates in petrochemical synthesis. In particular, alkylation of benzene or toluene with alkanes would be a new potential way to synthesize many important alkyaromatic products, such as ethylbenzene, xylenes, cumene, ethyltoluene, etc.

The catalytic synthesis of alkylaromatics from alkanes and benzene was reported by Schmerling and Vesely (2) for the Friedel–Crafts catalyst systems and then studied by Olah *et al.* (3) in superacidic media. The above catalysts showed high catalytic activity and selectivity. The major reaction products resulted from direct alkane addition to aromatics. However, these catalysts suffered from numerous, mainly environmental and corrosion drawbacks.

These drawbacks can be overcome by using solid catalysts. In view of this, over the past few years, there have been some efforts aimed at creating the heterogeneous systems for this process. In particular, zeolite-type solid acids were reported to produce alkylbenzenes from aromatics and light paraffins (4–8). However, these catalysts showed rather low selectivity toward the products of direct addition; instead, alkylaromatic products were formed from the fragments of alkane molecules and aromatic substrate (5–7). The reaction pathway leading to alkylaromatics in the presence of zeolites was found to be much more complicated than in the case of conventional acids (6, 7). Moreover, the reactivity of alkanes over zeolites was reported to be very low with respect to superacids and therefore high temperatures were required for this process (5, 7).

It has been demonstrated that zeolite reactivity in alkane activation can be improved significantly by modification with Pt, Ga, or Zn (9–11). Another possible way to increase conversion in the processes leading to H<sub>2</sub> release is to shift thermodynamic equilibria by continuous removal of hydrogen from the reaction zone. This could be achieved by addition of H<sub>2</sub> scavengers, such as hydride-forming materials, as demonstrated for the case of alkane dehydrogenation

<sup>1</sup> To whom correspondence should be addressed.

(12, 13), alcohol decomposition (14), and aromatization (14, 15) reactions.

In this paper, we report on benzene alkylation with propane on Pt-supported zeolites and oxides in the presence of an H<sub>2</sub> acceptor. The effects of the nature of support, its acidity, metal distribution, and addition of hydrogen scavenger are examined.

## EXPERIMENTAL

### 1. Materials

The MFI zeolite catalysts with SiO<sub>2</sub>/Al<sub>2</sub>O<sub>3</sub> ratios of 51, 104, and 325, designated in text as MFI-50, MFI-100, and MFI-300, were provided by UOP. CeO<sub>2</sub> and Al<sub>2</sub>O<sub>3</sub> were obtained from Rhône Poulenc.

The characteristics of initial and modified catalysts are given in Table 1.

H<sup>-</sup> forms and Na, H<sup>-</sup> forms of MFI zeolites were obtained by complete and partial ion exchange with NH<sub>4</sub>Cl aqueous solution, respectively. Ion exchange was followed by washing, drying, and calcination at 823 K for 5 h.

Pt/zeolite catalysts were prepared by ion exchange of NH<sub>4</sub><sup>+</sup> forms of corresponding zeolites with [Pt(NH<sub>3</sub>)<sub>4</sub>]Cl<sub>2</sub> aqueous solution. After ion exchange, samples were washed, dried at 333 K, calcined in the dry air flow at 773 K for 5 h, and reduced in the hydrogen flow at 723 K for 3 h.

For the MFI-300 sample with low ion exchange capacity, this procedure led to low Pt contents (Table 1). To obtain higher degrees of Pt incorporation in that sample, the Na<sup>+</sup> form of MFI-300 zeolite was exchanged with [Pt(NH<sub>3</sub>)<sub>4</sub>](OH)<sub>2</sub> aqueous solution. The sample was then washed, dried, calcined, and reduced as above.

Pt/CeO<sub>2</sub> and Pt/Al<sub>2</sub>O<sub>3</sub> catalysts were prepared by an incipient wetness impregnation method using a [Pt(NH<sub>3</sub>)<sub>4</sub>]Cl<sub>2</sub> aqueous solution. The samples were dried, calcined, and reduced as above.

Intermetallic compound Zr<sub>2</sub>Fe was prepared from 99.99% pure zirconium and iron components by nonconsumable electrode arc melting under a purified argon atmosphere. Sample was remelted five times to ensure its homogeneity. The hydrogen absorption capacity found for the sample prepared was 1.6 wt%, which is close to the data reported previously (16).

### 2. Characterization

The acidity of the catalysts was measured by temperature-programmed desorption (TPD) of ammonia. TPD NH<sub>3</sub> experiments were performed in a locally constructed apparatus. The catalyst (150 mg, 45 mesh particles) was loaded in a stainless steel microreactor connected online with a TC detector. The typical procedure for sample pretreatment before NH<sub>3</sub> adsorption included *in situ* activation at 773 K in a flow of dry air for 1 h and then in a flow of dry nitrogen or 1 h. Pt-containing samples were pretreated in a flow of high-purity Ar (99.998%) at 723 K for 1 h. NH<sub>3</sub> adsorption was carried out at ambient temperature in a flow of NH<sub>3</sub> diluted with N<sub>2</sub> (1 : 1) and purified on a column with granulated NaOH. The complete saturation of the samples with ammonia was reached within 30 min. Afterward, the weakly bound NH<sub>3</sub> was removed in a flow of dry He at 373 K for 30 min and the reactor was cooled to ambient temperature. The typical TPD experiment was carried out in a flow of dry He (30 ml/min), the temperature was increased linearly from 295 to 973 K, and the rate of heating was 8.5 K/min.

TABLE 1  
Characteristics of the Catalysts

Catalyst	SiO <sub>2</sub> /Al <sub>2</sub> O <sub>3</sub>	Na <sub>2</sub> O/Al <sub>2</sub> O <sub>3</sub>	Acid sites concentration (TPD NH <sub>3</sub> data), μmol g <sup>-1</sup>				Pt sites		
			a <sub>α</sub> <sup>a</sup>	a <sub>β</sub> <sup>a</sup>	a <sub>γ</sub> <sup>a</sup>	Total	Pt content, wt%	Average particle size, Å	
								STEM	H <sub>2</sub> adsorption
H-MFI-50	51	0.02	153	369	334	856	—	—	—
H-MFI-100	104	<0.01	168	120	141	429	—	—	—
Na,H-MFI-100	104	0.83	133	151	12	296	—	—	—
H-MFI-300	325	0.09	61	73	78	212	—	—	—
CeO <sub>2</sub>	—	—	n/d <sup>b</sup>	n/d	n/d	33	—	—	—
Al <sub>2</sub> O <sub>3</sub>	—	—	n/d	n/d	n/d	77	—	—	—
Pt/H-MFI-50	51	<0.01	168	230	188	586	0.29	9	9
Pt/H-MFI-100	104	<0.01	90	111	153	354	0.28	n/d	10
Pt(I)/H-MFI-300	325	<0.01	n/d	n/d	n/d	n/d	0.02	n/d	n/d
Pt(II)/H-MFI-300	325	<0.01	27	48	30	105	0.22	n/d	12
Pt/CeO <sub>2</sub>	—	—	n/d	n/d	n/d	90	0.30	n/d	14
Pt/Al <sub>2</sub> O <sub>3</sub>	—	—	n/d	n/d	n/d	77	0.30	9	9

<sup>a</sup> Amount of acid sites, corresponding to α, β, and γ peaks in NH<sub>3</sub> TPD profiles of the samples (α: E < 105 kJ/mol; β: 105 kJ/mol < E < 145 kJ/mol, γ: E < 145 kJ/mol).

<sup>b</sup> Not determined.

The acid sites distribution as a function of activation energies was determined according to the procedure described elsewhere (17).

*Pt contents* were determined by AE spectroscopy using a microwave plasma generator "Chromatron-1."

*The average sizes* of Pt particles were estimated by STEM and hydrogen adsorption measurements. STEM images were obtained on Vacuum Generators HB 601. Adsorption measurements were carried out on a standard static volumetric adsorption apparatus. The dispersion ( $D$ ) of Pt particles was determined as  $D = N_s/N_{\text{tot}}$ , where  $N_s$  corresponds to the fraction of the metal atoms exposed at the surface and  $N_{\text{tot}}$  to the total number of Pt atoms in the sample.  $N_{\text{tot}}$  was obtained from chemical analysis data, and  $N_s$  from isotherms of hydrogen adsorption using the following procedure. The sample was first reduced in  $\text{H}_2$  at 700 K, evacuated at that temperature, and then cooled to ambient temperature in a vacuum. The isotherm of hydrogen adsorption was then measured at ambient temperature. The linear part of the isotherm was extrapolated to zero pressure to obtain the sum of physisorbed and chemisorbed hydrogen. Physisorbed hydrogen was then evacuated at room temperature for 0.5 h and the back-sorption isotherm was measured. Subtraction of the second isotherm from the first gave a number of  $\text{H}_2$  molecules chemisorbed on the metal particles. Taking the stoichiometry of chemisorption as 1 H atom per 1 atom of metal (18), the number of chemisorbed hydrogen atoms gave the fraction of metal atoms exposed at the surface ( $N_s$ ). The size of the Pt particle was then calculated as described in (19).

### 3. Catalytic Tests

Catalytic tests were carried out in a continuous-flow catalytic unit. In a typical experiment, 0.8 g of the catalyst was placed in an up-flow, fixed-bed stainless steel reactor and pretreated in a flow of dry Ar (30 ml/min) at 723 K for 1 h; the system was then cooled to the reaction temperature. Ar flow was passed through the MnO/alumina indicator to verify the absence of oxygen in the stream.

When the catalytic system included two components (H-MFI + Pt/CeO<sub>2</sub> or Pt/MFI + Zr<sub>2</sub>Fe), zeolite was thoroughly mixed with the second component, and the mixtures were pressed into pellets, crushed, and size separated to give catalyst grains between 0.25 and 0.50 mm in diameter. In the case of the H-MFI + Pt/CeO<sub>2</sub> system, 0.8 g of zeolite was mixed with 0.8 g of Pt/CeO<sub>2</sub>. For the preparation of Pt/MFI + Zr<sub>2</sub>Fe catalyst, 0.8 g of Pt/MFI was ground with 2.4 g of intermetallic compound.

Benzene alkylation with propane was carried out at atmospheric pressure, in the temperature range of 573–773 K. The C<sub>3</sub>H<sub>8</sub>/C<sub>6</sub>H<sub>6</sub> molar ratio was  $\approx 1$ , and the weight hourly space velocity (WHSV) of the feed was varied from 0.2 to 7 h<sup>-1</sup>. The reaction products were analyzed online by GC using 50-m SE-30 and 50-m KCl/Al<sub>2</sub>O<sub>3</sub> capillary columns.

The selectivity to a specific reaction product was determined as the percentage of this product in total feed-free products.

The yield of propylbenzenes was determined as experimental conversion of reactants into propylbenzenes divided by equilibrium conversion of reactants into propylbenzenes. Equilibrium conversion was calculated for the system including benzene, propane, cumene, *n*-propylbenzene, and dihydrogen.

## RESULTS

### 1. Nature and Distribution of Acidic and Dehydrogenation Sites

The materials selected for the study involved three types of solids: neutral (CeO<sub>2</sub>), slightly acidic (Al<sub>2</sub>O<sub>3</sub>), and strongly acidic (MFI zeolites). The acidity was characterized by TPD of ammonia according to the procedure described above. The TPD profiles obtained and the acid sites distribution as a function of activation energies are presented in Figs. 1 and 2 and Table 1, respectively.

Cerium oxide which has been selected as a model of the neutral material is indeed characterized by the lowest amount of adsorption sites (Fig. 1, Table 1). The adsorption of ammonia on this sample is probably due to structural defects, which are always present on ceria.

On aluminum oxide, the amount of adsorption sites is a factor of 2 higher with respect to ceria. The origin of NH<sub>3</sub> adsorption in this case is most probably the Lewis acid sites of alumina.

Interestingly, the modification of CeO<sub>2</sub> and Al<sub>2</sub>O<sub>3</sub> with Pt results in different consequences. The TPD NH<sub>3</sub> profile of Pt/Al<sub>2</sub>O<sub>3</sub> is similar to those observed for Al<sub>2</sub>O<sub>3</sub> (Fig. 1). In contrast, Pt deposition on CeO<sub>2</sub> results in significant changes: a narrow peak at 480 K appears (Fig. 1) and the total amount of sites increases by a factor of 3 (Table 1). This observation suggests that Pt modifies the adsorption

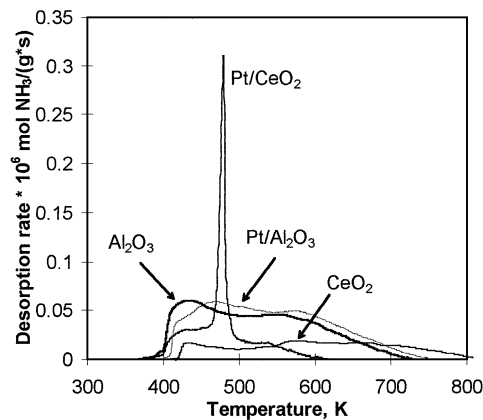


FIG. 1. TPD NH<sub>3</sub> profiles for oxide samples.

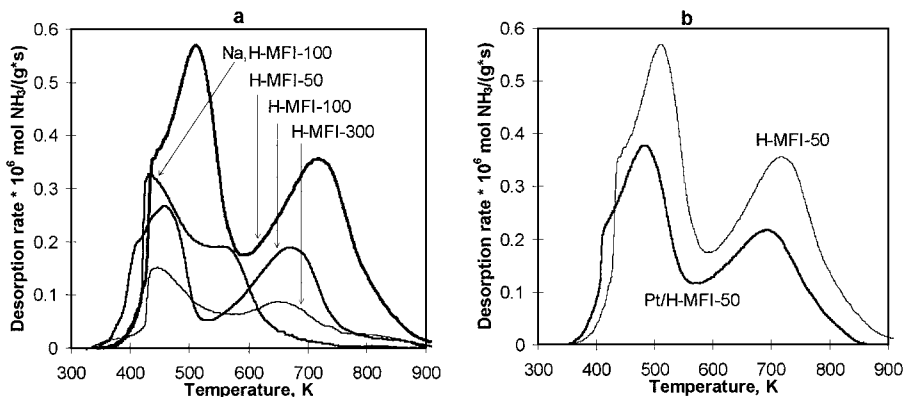


FIG. 2. TPD NH<sub>3</sub> profiles for zeolite samples.

sites of ceria, while the Lewis sites of alumina remain practically unchanged. Further experiments are needed to give an explanation for this phenomenon.

TPD NH<sub>3</sub> curves for H-MFI zeolites (Fig. 2a) are typical for this class of materials (20, 21). Three peaks at 350–450, 450–600, and 600–900 K, corresponding to weak, intermediate, and strong acid sites, are resolved. According to the classification proposed by Topsoe *et al.* (20), these peaks can be assigned to  $\alpha$ ,  $\beta$ , and  $\gamma$  sites, respectively. The intensity of the  $\gamma$  peak and the temperature of its maximum increase with the number of aluminum atoms in the framework (Table 1, Fig. 2a), in line with previous observations (20, 21). The highest concentration of the strongest  $\gamma$  sites was observed on the H-MFI-50 sample.

On the Na, H-MFI-100 sample, the  $\alpha$  peak gives the main contribution to the overall acidity, and the  $\beta$  peak is less essential, while the  $\gamma$  peak is absent in the TPD profile (Fig. 2a). Consequently, this sample exhibits mainly weak acid sites.

Pt deposition decreases the total amount of adsorbed ammonia on H-MFI samples by a factor of 1.5–2 but does not change significantly the acid sites distribution (Table 1, Fig. 2b). This effect could be either due to the partial blockage of zeolite channels by Pt particles or due to the interaction of Pt with the Brønsted acid sites of zeolites. Since the pore volume of the samples, measured by N<sub>2</sub> adsorption, does not change upon Pt deposition, the second hypothesis is more realistic. Hence, protonic sites of zeolites and aprotic sites of alumina show different behavior upon Pt deposition.

The amount and size distribution of dehydrogenation sites on Pt-containing samples is given in Table 1 and Fig. 3. For the most of the samples studied, Pt content is close to 0.3%. For H-MFI-300, two samples with different Pt contents of 0.02 and 0.22%, respectively, were prepared.

According to STEM and H<sub>2</sub> adsorption data (Table 1), the average Pt particle sizes do not change significantly within the range of samples studied and vary from 9 to

14 Å. STEM images suggest that Pt distribution is rather uniform. Moreover, on zeolite samples, Pt particles are shown to be inside of the channels (Fig. 3). Based on the latter observation and taking into account the dimensions of Pt particles (9 Å) and zeolite channels (5.5 Å), one can conclude that Pt particles are most probably located in zeolite channel intersections, where more space is available. Interestingly, the Brønsted acid sites of MFI are also located in zeolite channel intersections (22). Consequently, the dehydrogenation and acidic sites should be very close to each other in the MFI samples. This conclusion supports our interpretation of the effect of Pt on the acidity of H-MFI zeolites.

## 2. Benzene Alkylation with Propane over Acidic Zeolites

The study of the main regularities of benzene alkylation with propane was performed over H-MFI-50 catalyst. The variations of propane and benzene conversions with temperature and contact time are shown in Fig. 4.

The reaction starts at 573 K, the conversion of reactants being about 0.3%. In the range of 573–673 K, the conversion remains rather low. A further increase of the reaction temperature leads to a significant increase of activity and at 773 K, conversions of benzene and propane reach 37 and 63%, respectively (Fig. 4a).

The variations of propane and benzene conversions with contact time show linear dependences at 623 K (Fig. 4b). The maximum conversions reached at a contact time of 5 h were 7 and 11% for benzene and propane, respectively. It should be mentioned that at low temperatures (<673 K) and contact times (<1 h), the conversion of propane is close to benzene conversion, suggesting that the main reaction pathway is alkylation, while at higher temperatures and contact times conversion of neat propane contributes significantly to the overall reaction.

The major products observed include C<sub>1</sub>–C<sub>4</sub> gases, toluene (T), ethylbenzene (EB), isopropylbenzene (IPB), and *n*-propylbenzene (NPB). Others products detected

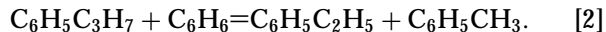


FIG. 3. STEM image for Pt/H-MFI-50 sample.

in smaller amounts involve alkyl- and polyalkylbenzenes, naphthalene, and its derivatives. The influence of temperature and contact time on the distribution of the main reaction products is shown on Fig. 5. At low temperatures (<623 K) and contact times (<0.5 h) propylbenzenes are the major reaction products. At higher temperatures and contact times, ethylbenzene and methane become the main products. A further increase of temperature to 700 K results in a decrease of ethylbenzene yields and an increase of conversion into toluene and ethane.

The analysis of the initial parts of kinetic curves presented in Fig. 5a suggests that propylbenzenes are the primary reaction products; however, they undergo rapid dealkylation or dismutation into ethylbenzene and toluene under our reaction conditions. Methane is also a primary product but the rate of its formation is much lower than in the case

of propylbenzenes. Ethylbenzene arises from both primary and secondary reactions which could be as follows:



Toluene is most probably formed only via the secondary route [2] as no ethane is observed as a primary product.

The comparison of the results obtained over the catalysts with different acidity is presented in Table 2.  $\text{CeO}_2$ ,  $\text{Al}_2\text{O}_3$ , and Na,H-MFI-100 materials do not show any activity in benzene alkylation with propane at 623 K. The activity of H-MFI zeolites increases with the number of strong acid sites on these samples. Indeed, almost linear correlation was obtained between propane conversion and the amount of  $\gamma$  sites (Fig. 6a). In contrast, no correlation was observed with

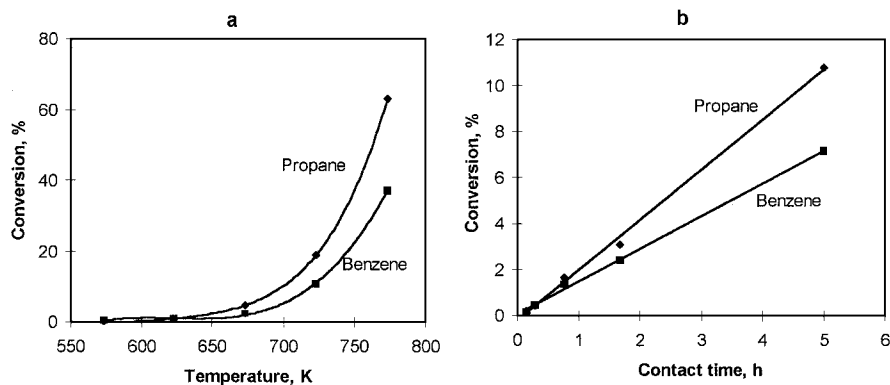


FIG. 4. Variation of benzene and propane conversions on H-MFI-50 with temperature at  $\text{WHSV} = 1.3 \text{ h}^{-1}$  (a) and with contact time at 623 K (b).

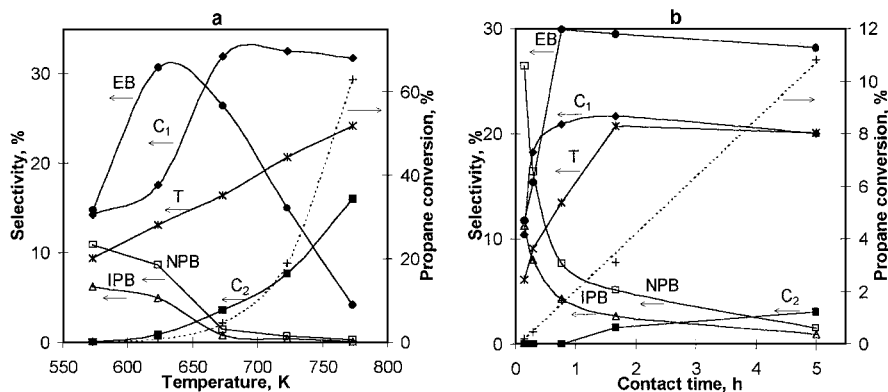


FIG. 5. Variation of product selectivity on H-MFI-50 with temperature at WHSV = 1.3 h<sup>-1</sup> (a) and with contact time at 623 K (b).

$\alpha$  and  $\beta$  sites as well as with the total amount of sites. These observations suggest that only strong Brønsted sites can activate propane, in line with the previous findings (9–11).

It should be mentioned that an increasing amount of  $\gamma$  sites favors methane and ethylbenzene formation at the expense of propylbenzenes, which leads to decreased selectivity in the alkylation process (Fig. 6b).

Consequently, on one hand, activation of propane needs strong acid sites, while on the other hand, these sites favor cracking at the expense of alkylation and lead to low selectivity toward the target process. To improve the catalyst activity and selectivity, the propane activation step should be modified. This could be achieved by addition of a dehydrogenation component and coupling of alkylation process with dehydrogenation, as was done previously for alkane isomerization (23, 24) and aromatization (9–11).

### 3. Benzene Alkylation with Propane over Pt-Supported Catalysts

Platinum metal was selected as the dehydrogenation component in our study. The results obtained on Pt-supported catalysts are presented in Tables 3 and 4.

Pt/CeO<sub>2</sub> is inactive in benzene alkylation (Table 3). The main process which takes place over this catalyst is propane dehydrogenation, the conversion of propane being less than 0.2%. Pt/Al<sub>2</sub>O<sub>3</sub> gives 2% propane conversion, but the main reaction product is also propene. Only small amounts of propylbenzenes are formed on this catalyst. This result confirms that Lewis acid sites are not active in alkylation.

Mixing of Pt/CeO<sub>2</sub> with acidic zeolites results in a tremendous increase of propane conversion (Table 3). The higher the acidity of the zeolite, the higher is the improvement. The maximum propane conversion achieved on Pt/CeO<sub>2</sub> + H-MFI-50 catalyst is 11.8%, which is 65 times higher than on neat Pt/CeO<sub>2</sub> and 14 times higher than on neat H-MFI-50. This result points to a complementary synergy between the actions of Pt and acidic sites in the overall alkylation process.

A comparison of the main products distribution on H-MFI-50 and mixed Pt/CeO<sub>2</sub> + H-MFI-50 catalysts at the same conversion level (~11%) is presented in Fig. 7. The following differences occur due to the addition of a dehydrogenation component. First, the reaction route leading to methane and ethylbenzene is suppressed in the presence of Pt/CeO<sub>2</sub>. Second, mixing with Pt/CeO<sub>2</sub> results in a 5-fold

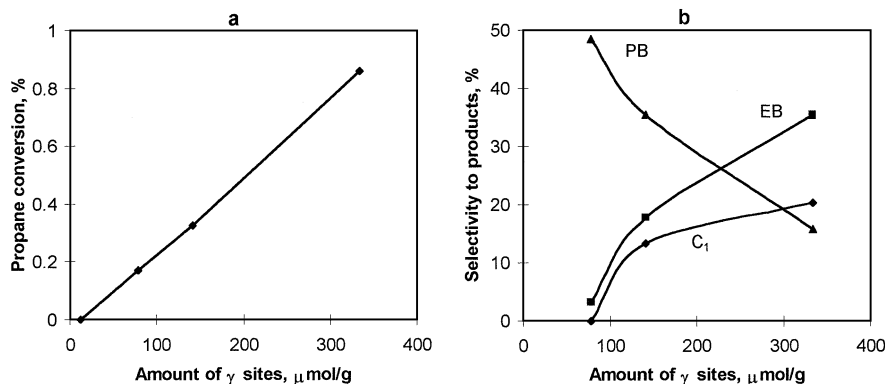


FIG. 6. Variation of propane conversion (a) and selectivity to the main products (b) with the amount of  $\gamma$  sites in MFI catalysts ( $T=623$  K, WHSV = 1.3 h<sup>-1</sup>, TOS = 1 h).

TABLE 2

Benzene Alkylation with Propane over the Catalysts with Different Acidity (WHSV = 1.3 h<sup>-1</sup>, 623 K, TOS = 1 h)

	CeO <sub>2</sub>	Al <sub>2</sub> O <sub>3</sub>	H-MFI-300	Na,H-MFI-100	H-MFI-100	H-MFI-50
Total propane conversion, %	0	0	0.17	0	0.32	0.86
Selectivity to hydrocarbons, mol%						
CH <sub>4</sub>	—	—	—	—	13.61	20.36
C <sub>2</sub> H <sub>6</sub>	—	—	—	—	—	0.99
C <sub>3</sub> H <sub>6</sub>	—	—	—	—	2.80	1.22
C <sub>4</sub> -C <sub>5</sub>	—	—	—	—	—	2.88
T	—	—	8.04	—	8.08	15.17
EB	—	—	3.12	—	17.66	35.52
IPB	—	—	17.60	—	13.07	5.79
NPB	—	—	30.90	—	22.12	10.04
C <sub>9</sub> -C <sub>11</sub>	—	—	31.60	—	5.83	—
Others	—	—	8.74	—	16.83	8.03

TABLE 3

Benzene Alkylation with Propane over Neat Pt-Supported Oxides and Mixed with Acidic Zeolites (WHSV = 1.3 h<sup>-1</sup>, 623 K, TOS = 1 h)

	Pt/CeO <sub>2</sub>	Pt/Al <sub>2</sub> O <sub>3</sub>	Pt/CeO <sub>2</sub> + H-MFI-300	Pt/CeO <sub>2</sub> + Na,H-MFI-100	Pt/CeO <sub>2</sub> + H-MFI-100	Pt/CeO <sub>2</sub> + H-MFI-50
Total propane conversion, %	0.18	1.91	1.26	0.77	2.15	11.84
Selectivity to hydrocarbons, mol%						
CH <sub>4</sub>	14.14	13.31	3.50	5.10	4.06	3.01
C <sub>2</sub> H <sub>6</sub>	—	5.79	0.40	0.46	2.77	15.98
C <sub>3</sub> H <sub>6</sub>	85.86	72.35	4.83	37.71	6.33	0.59
C <sub>4</sub> -C <sub>5</sub>	—	—	—	—	3.73	26.80
T	—	—	2.20	1.71	14.61	21.54
EB	—	—	3.54	2.49	17.39	11.40
IPB	—	6.90	29.68	22.86	13.75	4.93
NPB	—	1.65	40.74	10.30	25.33	6.61
C <sub>9</sub> -C <sub>11</sub>	—	—	15.11	8.81	3.36	1.67
Others	—	—	—	10.56	8.67	7.47

TABLE 4

Benzene Alkylation with Propane over Pt-Supported H-MFI Catalysts (WHSV = 1.3 h<sup>-1</sup>, 623 K, TOS = 1 h)

	Pt(I)/H-MFI-300	Pt(II)/H-MFI-300	Pt/H-MFI-100	Pt/H-MFI-50
Total propane conversion, %	0.45	6.62	22.99	44.56
Selectivity to hydrocarbons, mol%				
CH <sub>4</sub>	—	0.38	8.46	4.39
C <sub>2</sub> H <sub>6</sub>	—	4.91	13.03	27.83
C <sub>3</sub> H <sub>6</sub>	—	13.62	2.23	0.35
C <sub>4</sub> -C <sub>5</sub>	—	6.85	9.18	10.26
T	2.56	1.27	4.29	19.58
EB	2.56	0.88	2.28	1.37
IPB	35.90	23.28	8.54	1.58
NPB	48.72	36.60	16.90	3.24
C <sub>9</sub> -C <sub>11</sub>	—	3.86	21.52	7.73
Others	10.26	8.35	13.57	23.67

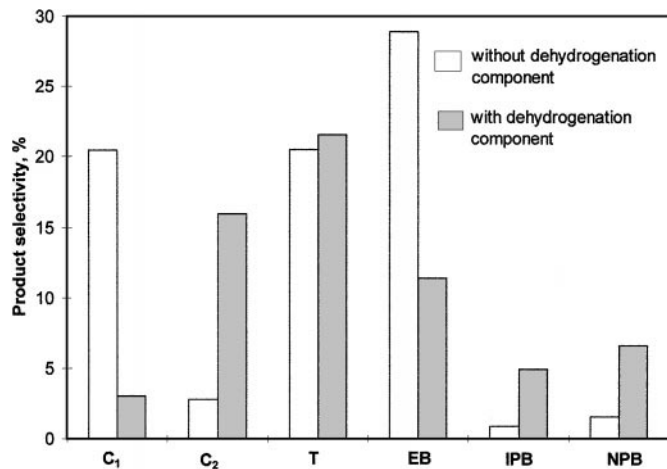


FIG. 7. Effect of mixing with Pt/CeO<sub>2</sub> on the product distribution over H-MFI-50 ( $T = 623$  K, propane conversion = 11%).

increase of the selectivity to target products. Hence, both the activity and the selectivity are increased upon Pt addition.

When Pt was deposited directly on the zeolite component the effect was even more pronounced (Table 4). Propane conversion increases 40–250 times with respect to neat Pt/CeO<sub>2</sub>, 40–70 times compared to pure acidic zeolites, and 4–10 times with respect to mixed Pt/CeO<sub>2</sub> + H-MFI systems. Propane conversion on the Pt/H-MFI-50 sample reaches 12% at 573 K and 44% at 623 K. On the H-MFI-50 catalyst, the same conversions can be reached at 700 and 750 K, respectively. Thus, addition of Pt to zeolite catalyst allows a decrease in the reaction temperature by more than 100 K, which is in line with the results obtained by Bragin *et al.* (4, 5).

The positive effect depends on the amount of Pt deposited on zeolite. The increase of Pt content from 0.02 (Pt(I)/H-MFI-300) to 0.22 (Pt(II)/H-MFI-300) leads to an order of magnitude increase of propane conversion (Table 4).

As in the case of mixed catalysts, direct Pt deposition suppresses methane formation and results in an increase of selectivity to propylbenzenes. It should be mentioned, however, that at high conversions, the process is accompanied by formation of significant amounts of polyalkylbenzenes, naphthalene, and its derivatives.

To conclude, both methods of Pt deposition lead to significant improvement of zeolite activity and selectivity. However, the best effect is obtained on Pt/H-MFI catalysts, on which Pt and acidic sites should be very close to each other and may compose a single bifunctional center.

#### 4. Benzene Alkylation with Propane on Pt-Supported Catalysts in the Presence of an H<sub>2</sub> Acceptor

It has been demonstrated that thermodynamic equilibria in reactions leading to H<sub>2</sub> release (dehydrogenation, aromatization, etc.) can be shifted by addition of hydrogen scavengers, such as O<sub>2</sub>, CO, or CO<sub>2</sub> (25, 26), or intermetallic compounds [12–15]. In this study, we applied a similar approach to benzene alkylation with propane.

Zr<sub>2</sub>Fe intermetallic compound was used as a hydrogen scavenger. The reaction was carried out at 623 K, WHSV = 1.3 h<sup>-1</sup>. The results are presented in Table 5 and Fig. 8.

The following observations can be made:

—Propane conversion increases 2–8 times upon addition of Zr<sub>2</sub>Fe; the effect is more pronounced on the catalysts with lower acidity (Tables 4 and 5).

—The catalysts which exhibit lower activity (Pt(I)/H-MFI-300 and Pt(II)/H-MFI-300) show stable behavior

TABLE 5

#### Quad Benzene Alkylation with Propane over Pt-Supported H-MFI Catalysts in the Presence of H<sub>2</sub> Acceptor (WHSV = 1.3 h<sup>-1</sup>, 623 K, TOS = 1 h)

	Pt(I)/H-MFI-300 + Zr <sub>2</sub> Fe	Pt(II)/H-MFI-300 + Zr <sub>2</sub> Fe	Pt/H-MFI-100 + Zr <sub>2</sub> Fe	Pt/H-MFI-50 + Zr <sub>2</sub> Fe
Total propane conversion, %	3.78	14.36	38.11	76.20
Selectivity to hydrocarbons, mol%				
CH <sub>4</sub>	0.37	0.24	5.16	5.72
C <sub>2</sub> H <sub>6</sub>	0.74	3.69	13.20	29.08
C <sub>3</sub> H <sub>6</sub>	9.23	12.31	4.59	0.77
C <sub>4</sub> –C <sub>5</sub>	1.48	11.83	20.50	9.67
T	0.74	1.04	4.66	11.66
EB	2.21	1.18	3.21	4.74
IPB	33.21	23.11	8.30	1.89
NPB	50.18	35.65	17.86	3.75
C <sub>9</sub> –C <sub>11</sub>	—	8.63	12.06	9.70
Others	1.84	2.32	10.46	23.02

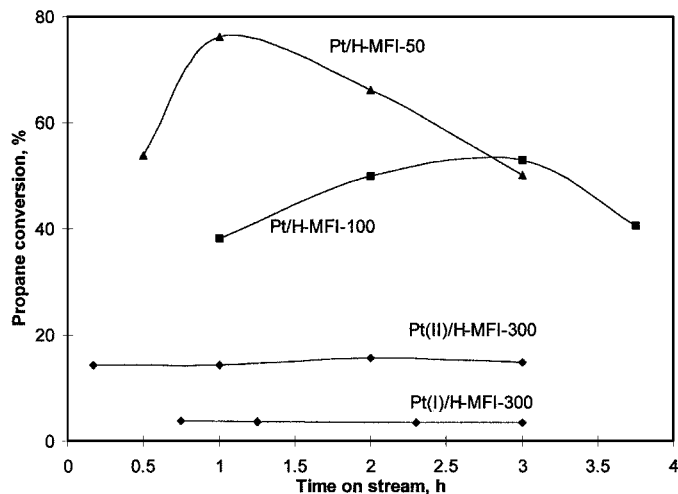


FIG. 8. Variation of propane conversion with time on stream over Pt/H-MFI catalysts mixed with  $Zr_2Fe$  ( $T = 623$  K, WHSV =  $1.3$  h $^{-1}$ , catalyst:  $H_2$  acceptor = 1 : 3).

during the time course of the reaction, while on more active catalysts (Pt/H-MFI-100 and Pt/H-MFI-50), the positive effect decreases with time on stream (Fig. 8). The latter observation could be due to saturation of hydrogen scavenger or due to fast deactivation of the catalytic system at high conversions. The estimation of the amounts of  $H_2$ , which evolve at the highest conversion levels under typical reaction conditions, have demonstrated that the  $H_2$  capacity of  $Zr_2Fe$  could be exhausted after 2–3 h on stream. Consequently, the first hypothesis seems to be more probable.

—Addition of an  $H_2$  acceptor does not change significantly the product distribution and selectivity to propylbenzenes remains the same as on neat catalyst (Tables 4 and 5).

## DISCUSSION

The results presented above and obtained in our previous studies (6, 7) suggest that interaction of propane with benzene over zeolite catalysts occurs via three main reaction pathways (Fig. 9) leading to (1) propylbenzenes and dihydrogen, (2) ethylbenzene and methane, (3) toluene and ethane. Under our experimental conditions ( $T > 573$  K), propylbenzenes are very unstable intermediate products, and convert into benzene and propene or react with benzene to give ethylbenzene and toluene. Apart from being involved in alkylation reactions, propane can also be dehydrogenated to propene which can undergo further oligomerization, isomerization, cracking alkylation, and aromatization reactions leading to long-chain oligomers, various alkylbenzenes, naphthalene, and its derivatives.

Thermodynamic calculations show (Fig. 10) that direct alkylation is not a favored reaction within the temperature range studied. In contrast, alkylation with the fragments

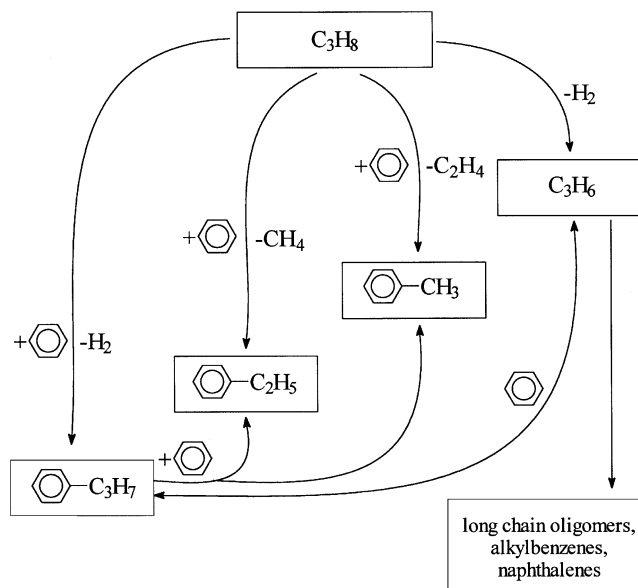


FIG. 9. Reaction network.

formed from alkane molecules is more favorable due to the contribution of the reaction pathways which allow cracking of alkane.

On nonmodified acidic zeolites, formation of ethylbenzene and methane was indeed the main reaction pathway (Table 2, Fig. 5). These catalysts showed the lowest overall conversion and selectivity to the products of direct addition.

Incorporation of Pt in the catalysts resulted in a significant increase of overall conversion and selectivity to propylbenzenes (Tables 3 and 4, Fig. 7). It should be emphasized that the effect was more pronounced on Pt/H-MFI systems than on Pt/CeO $_2$  + H-MFI mixed systems, suggesting that the mean distance between Pt and the acid site is very

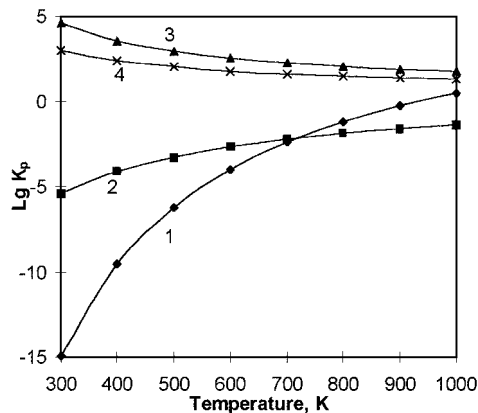


FIG. 10. Equilibrium constants as a function of temperature for the following reactions: (1)  $C_3H_8 = C_3H_6 + H_2$ ; (2)  $C_3H_8 + C_6H_6 = C_6H_5-C_3H_7 + H_2$ ; (3)  $C_3H_8 + C_6H_6 = C_6H_5-C_2H_5 + CH_4$ ; and (4)  $C_3H_8 + C_6H_6 = C_6H_5-CH_3 + C_2H_6$ .

important. The shorter the distance, the more active and selective is the catalyst. It appears that dehydrogenation and acidic sites work in synergy for propane activation and further alkylation.

Finally, addition of an H<sub>2</sub> acceptor allows the shift of thermodynamic equilibria and an increase in propane and benzene conversion at the same level of selectivity.

In Fig. 11, selectivity is plotted versus conversion for all the catalysts studied. Interestingly, all the data fell on four distinct curves, suggesting that all the catalysts can be subdivided into four groups according to the mechanisms operating on them:

(I) Pure acidic catalysts (H-MFI).

(II) Mixed catalysts (Pt/CeO<sub>2</sub> + H-MFI), which consist of metal supported on neutral material and an acidic component. These catalysts include both dehydrogenation and acidic centers but the mean distance between these centers is rather long.

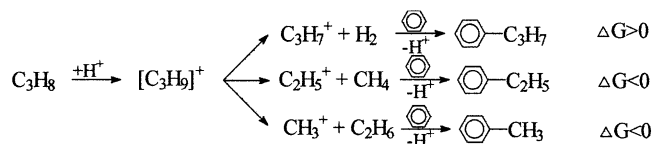
(III) Bifunctional catalysts (Pt/H-MFI), which involve Pt supported directly on acidic material. On these catalysts,

dehydrogenation and acidic centers are very close to each other and can act in synergy as combined bifunctional centers.

(IV) Bifunctional catalysts with an H<sub>2</sub>-acceptor (Pt/H-MFI + Zr<sub>2</sub>Fe), where the later works as a scavenger for hydrogen molecules formed during the reaction.

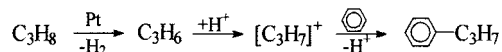
The following mechanistic pathways can be proposed to account for the results obtained for each group of catalysts:

—On acidic catalysts (group I) selectivity to propylbenzenes is very low. High amounts of CH<sub>4</sub> observed at low propane conversion point to a carbonium ion mechanism of propane activation on such catalysts [7, 27–29]. This mechanism involves propane protonation on the strong Brønsted sites of H-MFI catalysts and the formation of a carbonium ion type transition state, which may then evolve in three different ways leading to propyl-, ethyl-, and methylcarbenium ions, which further alkylate benzene to give propyl-, ethyl-, and methylbenzenes, respectively:



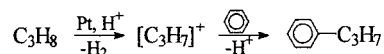
According to our data, the second route leading to ethylbenzene and methane is predominant on this type of catalysts.

—On mixed catalytic systems (group II) selectivity to methane decreases and propene appears in products in significant amounts. These observations suggest that on such catalysts propane activation preferentially occurs via its dehydrogenation to propene and dihydrogen. Metal (Pt) sites are most probably responsible for this step. Propene is further protonated on acid sites to give propenium ion which can alkylate benzene leading to propylbenzenes:



Propene formed on the first step can also participate in side reactions (oligomerization, aromatization, etc.) leading to a variety of by-products (Fig. 9). Propylbenzenes can undergo secondary reactions giving benzene and propene or ethylbenzene and toluene.

—On bifunctional catalysts (group III) propane dehydrogenation and protonation may take place on a metal-acidic center, which results in direct benzene alkylation:



As in the previous case, the products of direct addition can undergo dealkylation and dismutation reactions leading to benzene and propylene or toluene and ethylbenzene, respectively. Of course, one cannot exclude the existence of

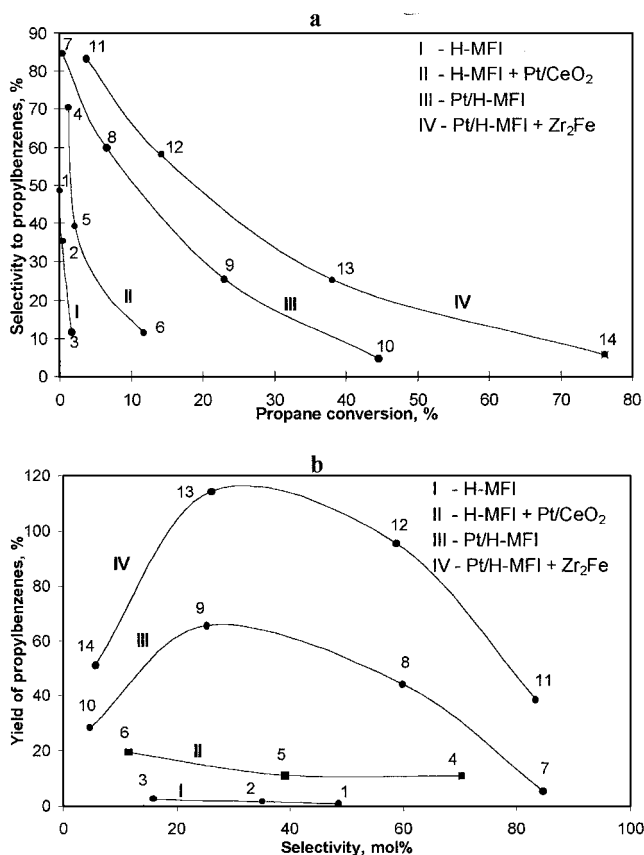
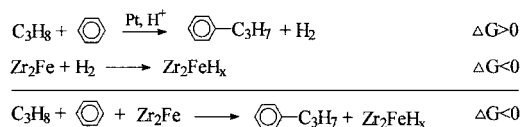


FIG. 11. Selectivity versus conversion (a) and yield versus selectivity (b) plots: (1) H-MFI-300; (2) H-MFI-100; (3) H-MFI-50; (4) H-MFI-300 + Pt/CeO<sub>2</sub>; (5) H-MFI-100 + Pt/CeO<sub>2</sub>; (6) H-MFI-50 + Pt/CeO<sub>2</sub>; (7) Pt(I)/H-MFI-300; (8) Pt(II)/H-MFI-300; (9) Pt/H-MFI-100; (10) Pt/H-MFI-50; (11) Pt(I)/H-MFI-300 + Zr<sub>2</sub>Fe; (12) Pt(II)/H-MFI-300 + Zr<sub>2</sub>Fe; (13) Pt/H-MFI-100 + Zr<sub>2</sub>Fe; (14) Pt/H-MFI-50 + Zr<sub>2</sub>Fe.

separated acidic and Pt sites on Pt-MFI catalysts along with bifunctional metal–acidic centers. On the separated sites, a mechanism similar to those proposed for mixed catalytic systems should be realized.

—Finally, when the reaction is carried out on bifunctional catalysts in the presence of an H<sub>2</sub> acceptor (group IV), the reaction mechanism is the same as in the previous case but thermodynamic equilibrium is shifted toward formation of propylbenzenes:



The results show that an H<sub>2</sub> acceptor (Zr<sub>2</sub>Fe) influences only the initial reaction step and does not participate in the other reactions. As a result, the product distribution remains as on the neat catalyst, while conversion increases 2–8 times.

To compare the activity of various catalysts and to select the best catalytic systems among those studied, the yields of propylbenzenes were determined as described in the Experimental part and plotted versus selectivity. The results are presented in Fig. 11b. The highest yields of 66–44% are observed on Pt/H-MFI-100 and Pt(II)/H-MFI-300, catalysts. Addition of Zr<sub>2</sub>Fe shifts the thermodynamic equilibrium and allows for a 2-fold increase of the yield. The highest yield of 114% with respect to equilibrium is observed on (Pt/H-MFI-100 + Zr<sub>2</sub>Fe); however, selectivity to propylbenzenes is rather low (26%) on this catalytic system. On (Pt(II)/MFI-300 + Zr<sub>2</sub>Fe), the yield is only slightly lower (96%), however, selectivity to propylbenzenes increases 2 times and reaches 60%.

## CONCLUSION

Interaction of benzene with propane over zeolite catalysts proceeds via three main reaction pathways leading to (1) propylbenzenes and dihydrogen, (2) ethylbenzene and methane, and (3) toluene and ethane. Under our experimental conditions (*T* > 573 K), propylbenzenes are very unstable and are converted into benzene and propene or interact with benzene to give ethylbenzene and toluene.

On acidic H-MFI zeolites, the major reaction route is conversion into methane and ethylbenzene. The products of direct addition are observed only in small amounts at low temperatures (<650 K), when the conversion is very low (<2%). The results observed are accounted for on the basis of carbonium ion mechanistic pathway including propane protonation on strong Brønsted sites, and formation of proponium ion, which is further decomposed predominantly into CH<sub>4</sub> and C<sub>2</sub>H<sub>5</sub><sup>+</sup>; H<sub>2</sub> and C<sub>3</sub>H<sub>7</sub><sup>+</sup> or C<sub>2</sub>H<sub>6</sub> and CH<sub>3</sub><sup>+</sup> are

also formed in small amounts. The reactions of C<sub>2</sub>H<sub>5</sub><sup>+</sup>, C<sub>3</sub>H<sub>7</sub><sup>+</sup>, and CH<sub>3</sub><sup>+</sup> carbenium ions with benzene lead to ethylbenzene, propylbenzenes, and toluene, respectively.

Incorporation of Pt into the catalysts results in a significant increase of the overall conversion and selectivity to propylbenzenes. It is demonstrated that on Pt-containing systems, the reaction mechanism is bifunctional: both dehydrogenation and acidic sites act in synergy for propane activation, leading preferentially to H<sub>2</sub> and C<sub>3</sub>H<sub>7</sub><sup>+</sup> and further to propylbenzenes. The effect is more pronounced on Pt/H-MFI systems than on Pt/CeO<sub>2</sub> + H-MFI mixed systems, due to the shorter mean distance between the acidic and dehydrogenation sites on the former.

Addition of an H<sub>2</sub> scavenger shifts the thermodynamic equilibrium of the reaction and allows for further improvement of activity and selectivity. The best result is observed on the (Pt(II)/H-MFI-300 + Zr<sub>2</sub>Fe) catalytic system, on which the yield of propylbenzenes reaches 96% with respect to equilibrium and selectivity to propylbenzenes is about 60%.

## REFERENCES

- Shilov, A. E., "Activation of Saturated Hydrocarbons by transition Metal Complexes," p. 304. Reidel, Dordrecht, 1984.
- Schmerling, L., and Vesely, J. A., *J. Org. Chem.* **38**, 312 (1973).
- Olah, G. A., Schilling, P., Staral, J. S., Halpern, Yu., and Olah, J. A., *J. Am. Chem. Soc.* **97**, 6807 (1975).
- Bragin, O. V., Vasina, T. V., Isaev, S. A., and Minachev, Kh. M., *Izv. Akad. Nauk USSR, Ser. Khim.* **7**, 1682 (1987).
- Isaev, S. A., Vasina, T. V., Bragin, O. V., *Izv. Akad. Nauk USSR, Ser. Khim.* **10**, 2228 (1991).
- Ivanova, I. I., Blom, N., and Derouane, E. G., *J. Mol. Catal.* **109**, 157 (1996).
- Ivanova, I. I., and Fajula, F., *Proc. 12th Int. Zeolite Conf.* **IV**, 2273 (1998).
- Kato, S., Nakagawa, K., Ikenaga, N., and Suzuki, T., *Chem. Lett.*, 207 (1999).
- Guisnet, M., Gnep, N. S., and Alario, F., *Appl. Catal.* **89**, 1 (1992).
- Ono, Y., *Catal. Rev. Sci. Eng.* **34**, 179 (1992).
- Derouane, E. G., Abdul Hamid, S. B., Ivanova, I. I., Blom, N., and Hojlund-Nielsen, P. E., *J. Mol. Catal.* **86**, 371 (1994).
- Fanelli, A. J., Maeland, A. J., Rosan, A. M., and Crissey, R. K., *J. Chem. Soc., Chem. Commun.* **8** (1985).
- Imai, H., Tagawa, T., and Kuraishi, M., *Mater. Res. Bull.* **20**, 511 (1985).
- Imai, H., Tagawa, T., and Nakamura, K., *Appl. Catal.* **62**, 348 (1990).
- Chetina, O. V., Vasina, T. V., Lunin, V. V., and Bragin, O. V., *Catal. Today* **13**, 639 (1992).
- Van Essen, R. M., and Buschow, K. H. J., *J. Less Common Met.* **64**, 277 (1979).
- Yushchenko, V. V., *Russ. J. Phys. Chem.* **71**, 547 (1997).
- O'Rear, D. J., Loffler, D. G., and Boudart, M., *J. Catal.* **121**, 131 (1990).
- Scholten, J. J. F., in "Preparation of Catalysts II" (B. Delmon, P. Grange, P. Jacobs, and G. Poncelet, Eds.), p. 685. Elsevier Scientific, New York, 1979.
- Topsoe, N. Y., Pedersen, K., and Derouane, E. G., *J. Catal.* **70**, 41 (1981).

21. Meshram, N. R., Hegde, S. G., Kulkarni, S. B., and Ratnasamy, P., *Appl. Catal.* **8**, 359 (1983).
22. Jacobs, P., von Ballmoos, R., *J. Phys. Chem.* **86**, 3050 (1982).
23. Maxwell, L. E., and Stork, W. H. G., *Stud. Surf. Sci. Catal.* **58**, 575 (1991).
24. Yashima T., Wang, Z. B., Kamo, A., Yoneda, T., and Komatsu, T., *Catal. Today* **29**, 279 (1981).
25. Iglesia, E., and Baumgartner, J. E., *Catal. Lett.* **21**, 55 (1993).
26. Meitzner, G. D., Iglesia, E., Baumgartner, J. E., and Huang E. S., *J. Catal.* **140**, 209 (1993).
27. Haag, W. O., and Dessau, R. M., in "Proceedings, 8th International Congress on Catalysis, Berlin, 1984," p. 305. Dechema, Frankfurt-am-Main, 1984.
28. Krannila, H., Haag, W. O., and Gates, B. C., *J. Catal.* **135**, 115 (1992).
29. Ivanova, I. I., Pomakhina, E. B., Rebrov A. I., and Derouane, E. G., *Topics Catal.* **6**, 49 (1998).